JACS
JOURNAL OF THE AMERICAN CHEMICAL SOCIETY

Article

pubs.acs.org/JACS

Monodisperse Uni- and Multicompartment Liposomes

Nan-Nan Deng, Maaruthy Yelleswarapu, and Wilhelm T. S. Huck*

Radboud University, Institute for Molecules and Materials, Heyendaalseweg 135, 6525 AJ Nijmegen, The Netherlands

Supporting Information

ABSTRACT: Liposomes are self-assembled phospholipid vesicles with great potential in fields ranging from targeted drug delivery to artificial cells. The formation of liposomes using microfluidic techniques has seen considerable progress, but the liposomes formation process itself has not been studied in great detail. As a result, high throughput, high-yielding routes to monodisperse liposomes with multiple compartments have not been demonstrated. Here, we report on a surfactant-assisted microfluidic route to uniform, single bilayer liposomes, ranging from 25 to 190 μm, and with or without multiple inner compartments. The key of our method is the precise control over the developing interfacial energies of complex W/O/W emulsion systems during liposome formation, which is achieved via an additional surfactant in the outer water phase. The liposomes consist of single bilayers, as demonstrated by nanopore formation experiments and confocal fluorescence microscopy, and they can act as compartments for cell-free gene expression. The microfluidic technique can be expanded to create liposomes with a multitude of coupled compartments, opening routes to networks of multistep microreactors.

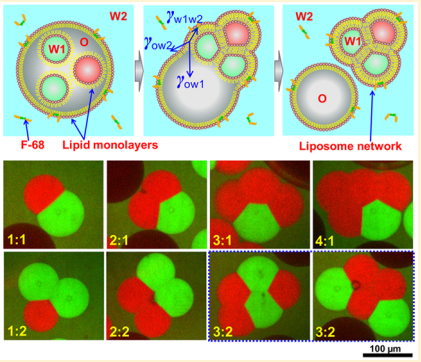

INTRODUCTION

There has been a significant interest in the use of liposomes, self-assembled phospholipid vesicles composed of bilayer membranes, in fields as diverse as targeted drug delivery,[1,2] membrane protein science,[3−5] bioreactors[6−8] and biosensors.[9,10] Cell-sized liposomes that encapsulate biomolecules and incorporate biological functions provide a versatile mimic of certain aspects of living cells, as exemplified by work showing RNA replication,[11−13] in vitro transcription and translation of gene networks,[6,14−16] and organization of cell division machinery in liposomes.[17−24]

However, conventional methods to synthesize lipid vesicles, such as extrusion through porous membranes,[25] electroformation,[26] reverse phase evaporation,[27] droplet emulsion transfer,[28] freeze-drying,[29] hydration or swelling,[30,31] give low yields, lead to polydisperse liposomes and show inefficient encapsulation.[32,33] Microfluidics offers a route to create uniform liposomes templated from either water-in-oil (W/O) single emulsion drops[34−37] or water-in-oil-in-water (W/O/W) double emulsion drops.[22,38−42] In the single emulsion method, lipid-stabilized W/O emulsion drops are prepared and subsequently transferred to a water phase via centrifugation or specially designed microchannels,[34,35,37] to obtain lipid bilayers. However, this route is typically very low-yielding, with 95−99% of liposomes bursting as they cross into the aqueous phase.[33] By contrast, double emulsion-templated methods based on fluid shearing,[22,38,39] pulsed jetting[40,41] or transient membrane ejection,[42] offer robust high-throughput production of monodisperse vesicles with high encapsulation efficiency.[32,33] However, these strategies crucially rely on the ultrathin-shelled double emulsions as templates, requiring more complicated device design and routes that are sensitive to the operating conditions or the materials being used, and the resultant vesicles often contain lipid reservoirs or residual oil in the lipid membranes.[39,40] Although recent work has improved the quality of the liposomes via emulsion dewetting,[22] the complete dewetting of double emulsion drops to form liposomes has not been studied in detail. Furthermore, the controlled formation of liposomes with multiple compartments has not been achieved, as the thin-shelled emulsion templates containing multicores are unstable and suffer from strong capillary forces that lead to the coalescence of inner compartments.[43,44] This limitation has hindered progress in the application of such multicompartment systems in coupled microreactors,[45,46] or complex liposome networks.[47−50]

In this paper, we report on a surfactant-assisted microfluidic strategy for assembling multicompartment liposomes from double emulsions. The key to the successful formation of monodisperse, stable and structured liposomes is control over the dewetting process. Dewetting phenomena of double emulsions are dominated by interfacial energies; a fact that has been utilized to prepare polymersomes including multicompartment structures.[51−53] However, controlled dewetting of double emulsions to form liposomes (single or multicompartmental) has not been achieved thus far, because simply replacing diblock copolymers (for example, poly(ethylene glycol)-*b*-poly(lactic acid)) with phospholipids in the polymersome preparation systems cannot trigger dewetting transitions.[39] Here, we use a triblock copolymer surfactant, Pluronic F-68, to adjust interfacial energies in the W/O/W emulsion system to ensure the complete dewetting and formation of oil-

Received: February 25, 2016
Published: May 31, 2016

DOI: 10.1021/jacs.6b02107
J. Am. Chem. Soc. 2016, 138, 7584−7591

free monodisperse liposomes with both single and multiple compartments. By changing the dimensions of the templates, liposomes ranging from 20 to 200 μm in diameter can be easily formed in capillary microfluidic devices. By changing the concentration of surfactant, the dewetting time can be adjusted from less than 1 min to about 3 h. Finally, we demonstrate that our method is compatible with cell-free gene expression and that the resulting liposomes are unilamellar vesicles, allowing the insertion of membrane proteins such as melittin and alpha-hemolysin into the membranes. This innovative approach for fabricating controllable uniform liposomes in high yield and high throughput can facilitate research on the use of liposomes as cell-like biodevices or as advanced delivery methods.

RESULTS AND DISCUSSION

Surfactant-Controlled Dewetting of W/O/W Emulsion Drops. The dewetting of double emulsions is determined by the spreading coefficient that is defined as $S_i = \gamma_{jk} - (\gamma_{ij} + \gamma_{ik})$, where γ_{ij} is the interfacial tension between fluids i and j.[54,55] To illustrate, we take W1/O/W2 double emulsions for example: when $S_o < 0$, i.e.,

$$\gamma_{w1w2} - (\gamma_{ow1} + \gamma_{ow2}) < 0 \quad (1)$$

the dewetting will occur spontaneously to minimize the total interfacial energies (from Figure 1a1 to Figure 1a2). However, a

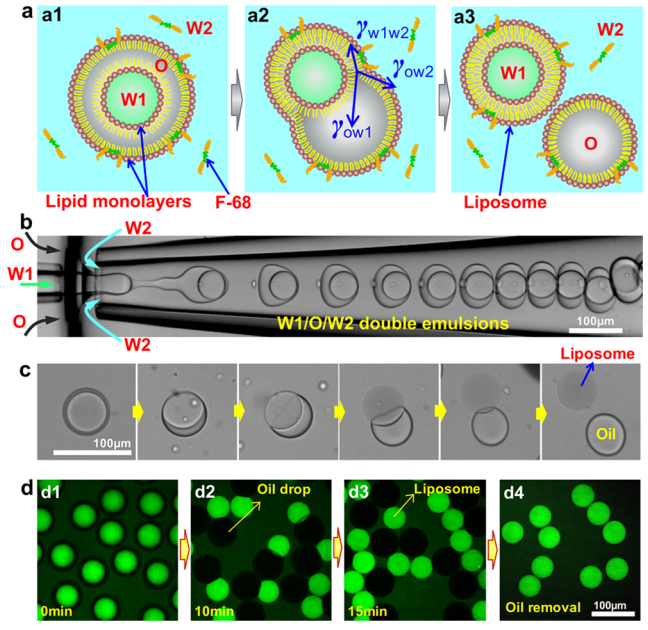

Figure 1. (a) Cartoon of surfactant-assisted assembly of liposome from dewetting of double emulsion drop. (b) Preparation of W/O/W double emulsions in a microcapillary-based device. (c,d) Time-serial optical (c) and confocal (d) images of the complete dewetting process (d1–d3) with liposomes separating from residual oil droplets (d4). W1, W2 and O stand for inner water phase, outer water phase and oil phase, respectively. Scale bars are 100 μm.

complete dewetting of phase O over phase W1 (from Figure 1a2 to Figure 1a3) also requires $S_{w1} < 0$, i.e.,

$$\gamma_{ow2} - (\gamma_{ow1} + \gamma_{w1w2}) < 0 \quad (2)$$

and $S_{w2} > 0$, i.e.,

$$\gamma_{ow1} - (\gamma_{ow2} + \gamma_{w1w2}) > 0 \quad (3)$$

From eq 1, 2, and 3, we conclude the criterion for complete dewetting of W1/O/W2 emulsion drops is the eq 3. Only if $S_{w2} > 0$, will the dewetting process go to completion, resulting in separated aqueous (W1) and oil (O) droplets. Moreover, higher S_{w2} values result in higher driving forces for dewetting, and thus faster dewetting transitions. This criterion agrees well with the adhesion energy ΔF derived from the Young–Dupre equation of the droplet system, $\Delta F = \gamma_{ow2} + \gamma_{w1w2} - \gamma_{ow1}$.[56] When $S_{w2} > 0$, ΔF is negative, meaning that there is no adhesion energy between the two drops. In this paper, we utilize a triblock copolymer surfactant, Pluronic F-68 (see Supporting Information for selection of surfactants), to adjust the interfacial energies of phospholipid stabilized W/O/W emulsion drops, ensuring their complete dewetting and formation of oil-free monodisperse liposomes with multiple compartments.

W/O/W double emulsion drops were prepared in a glass capillary microfluidic device as shown in Figure 1b (Movie S1, see Experimental Section for details about the device). Typically, the inner water phase (W1), middle oil phase (O) and outer water phase (W2) consisted of an aqueous solution with 8.0 wt % polyethylene glycol (PEG) and 2.0 wt % poly(vinyl alcohol) (PVA), a mixture of chloroform and hexane (40:60, v/v) containing 1.0–5.0 mg mL^{-1} L-α-phosphatidylcholine (egg PC), and a 10.0 wt % PVA and 0.1–5.0 wt % F-68 solution, respectively. PEG and PVA are used here to improve emulsion preparation and stability. The freshly prepared double emulsions were collected in a sealed container and observed immediately. To observe the dewetting process and liposomes clearly, methylene blue or fluorescein isothiocyanate-dextran (FITC-Dextran) were added in the inner phase in some experiments. As illustrated in Figure 1c and d, the dewetting process was recorded using optical or confocal fluorescence microscopy; the oil shells gradually dewetted from the interior drops within 15 min at a concentration of 0.3 wt % F-68, ultimately forming completely separated liposomes and oil drops with excess lipids (Figure S1 and Movie S2).

This surfactant-assisted complete dewetting can be explained by careful analysis of the role of the surfactants. Once the W1/O/W2 emulsion drops are formed, lipids in the shell will adsorb to both internal and external water–oil interfaces to form two lipid monolayers (Figure 1a1). Meanwhile, the surfactant F-68 in W2 phase also adsorbs to the external water–oil interface (Figure 1a1), which further decreases interfacial tensions between O–W2 phases (γ_{ow2}) during evaporation of the chloroform fraction of the oil phase. For example, when the concentration of F-68 is 0.5 wt %, γ_{ow2} reduces from 0.63 mN m^{-1} to 0.28 mN m^{-1} as the chloroform fraction decreases from 40 vol % to 30 vol % (Table S1). In the absence of F-68, the corresponding values of γ_{ow2} are 0.59 mN m^{-1} and 0.45 mN m^{-1}, respectively (Table S2). Chloroform is a good solvent for lipids but also more soluble in water than hexane (solubility: chloroform 8 g L^{-1}, hexane 13 mg L^{-1} at 20 °C).[53] Chloroform diffuses from the oil shell into the outer water quickly and evaporates, making the shell a hexane-rich poor solvent for lipids, which induces an attractive interaction between the two lipid monolayers. With assistance of F-68, the interfacial tension between the two lipid monolayers (γ_{w1w2}) also decreases sharply from ≥0.78 mN m^{-1} (Table S2) to nearly 0 mN m^{-1} (Tables S1 and S3) at 30 vol % chloroform. The combination of interfacial tensions leads to a negative S_o (S_o = −0.61 and −0.51 when the surfactant concentration are 0.5 and 2.0 wt % at 30 vol % chloroform, respectively, see Tables S1 and S3); as a

DOI: 10.1021/jacs.6b02107
J. Am. Chem. Soc. 2016, 138, 7584–7591

result, the oil is expelled from the shell, and the two lipid monolayers stick together, forming a lipid bilayer membrane (Figures 1c second image, S1b). When the combination of interfacial tensions makes a positive S_{w2} (S_{w2} = 0.05 and 0.15 when the surfactant concentrations are 0.5 and 2.0 wt % at 30 vol % chloroform, respectively, see Tables S1 and S3), the inner drops will entirely dewet from the oil drops, forming intact liposomes (Figures 1c last image, 1d3 and S1c). As a control, W/O/W emulsions without F-68 were also prepared. In absence of F-68, these emulsions are very stable and but do not undergo the dewetting transition (Figure S2), because in this case S_o is always positive regardless of the chloroform fraction (Table S2). Importantly, the unwanted residual oil droplets formed after dewetting can be easily removed from liposome samples by exploiting the density differences in the system (Figure 1d4 and S3, see Experimental Section for details).

Our method for fabricating liposomes gives control over the dewetting time and liposome dimensions, as well as high yields over a range of experimental conditions. By changing the concentration of F-68 in the outer water phase, the dewetting time can be adjusted. As Figure 2a shows, when the

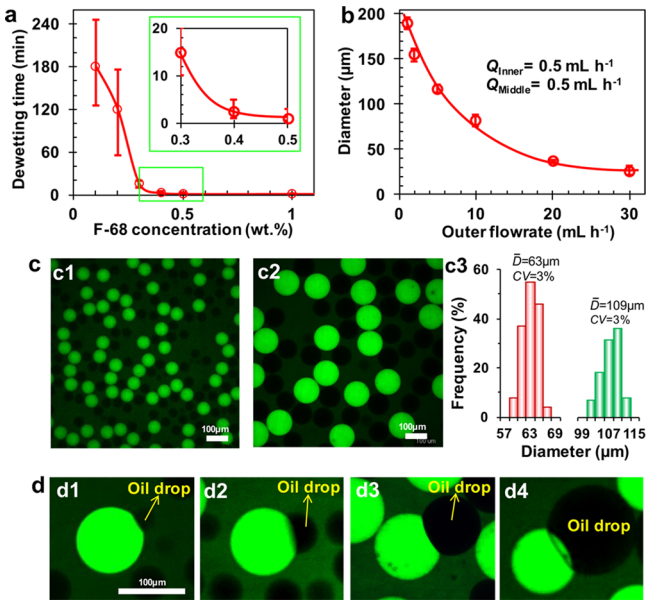

Figure 2. (a) Dewetting time is controlled by the concentration of F-68 in outer phase. (b) Dependence of the outer flow rate (Q_{Outer}) on the liposome diameter (D) as Q_{Middle}/Q_{Inner} is fixed at 0.5 mL h^{-1}/0.5 mL h^{-1}. (c) Confocal images of as-prepared liposomes in diameters of 63 (c1) and 109 μm (c2); (c3) the size distribution of liposomes in b1 and b2 (150 liposomes measured). (d) Successful dewetting of double emulsion drops with different shell thicknesses. Fluorescent liposomes contain FITC-dextran inside. Scale bars are 100 μm.

concentration of F-68 increases from 0.1 wt % to 1.0 wt %, the dewetting time will decrease sharply from 3 h to about 1 min. However, when the concentration of F-68 is as high as 5.0 wt %, the interfacial tension between W2 and O phases (γ_{ow2}) is as low as 0.1 mN m^{-1}, leading to unwanted emulsification and adhesion of the oil shells (Figure S4). We note that the preferable concentration of F-68 is between 0.3 and 1 wt %. The size of liposomes can be varied by tuning the flow rates. Figure 2b shows changes in liposome diameters from 190 to 25 μm as the outer flow rate (Q_{Outer}) increases from 0.5 mL h^{-1} to 30 mL h^{-1}, keeping the inner and middle phase flow rates (Q_{Inner} and Q_{Middle}) both fixed at 0.5 mL h^{-1}. By replacing the egg PC with other lipids or lipid mixtures, diverse liposomes composed of 1,2-dioleoyl-*sn*-glycero-3-phosphocholine (DOPC), 1,2-dimyristoyl-*sn*-glycero-3-phosphocholine (DMPC), 1,2-diphytanoyl-*sn*-glycero-3-phosphocholine (DPhPC), *E. coli* lipids or mixtures of egg PC and cholesterol were achieved (Figure S5). Remarkably, the droplet production rate can be as high as 1 kHz with a yield of liposomes as high as 94% (Figure S6), As-prepared liposomes are extremely uniform. Figure 2c shows the mean diameters of liposomes are 63 and 109 μm (Figure 2c1 and 2c2, respectively) and their coefficients of variation are both 3% (Figure 2c3). Importantly and in contrast to previously reported methods based on dewetting of double emulsions, the surfactant controlled dewetting is a spontaneous process and does not rely on specific solvent ratios of chloroform and hexane (Figure S7) nor the application of shear flows. Liposomes formed in our method therefore do not exhibit residual oil and lipid reservoirs (Figures 1d3 and S1c). To further demonstrate this, we added 1 mol % (to egg PC) labeled lipid, 1,2-dimyristoyl-*sn*-glycero-3-phosphoethanolamine-*N*-(lissamine rhodamine B sulfonyl) (ammonium salt) (Rh-PE) in the middle oil to visualize the bilayer membranes of resultant liposomes, in which the fluorescent lipids distribute homogeneously in the liposome boundaries (Figure S8). After removing residual oil drops, we characterized the liposomes by using gas chromatography. Results show that the signals of chloroform and hexane are too weak to identify, indicating that there is (almost) no oil left in the liposome sample (Figure S9). In addition, our method is independent of the thickness of the oil shells of the emulsion templates. Figures 2d1–d4 show liposomes with the same size formed from double emulsions with oil shell thickness ranging from 1 μm, to 3 μm, to 14 μm and to 36 μm, respectively. This controllability makes it possible to create multicompartment liposomes from double emulsions.

The key to the successful, complete dewetting of double emulsions to form liposomes is the control of interfacial energies using surfactants. In our case, this surfactant may adhere to the outer bilayer leaflet after liposome formation as the interaction between PEO–PPO–PEO triblock copolymers including F-68 and lipid bilayers has been studied in detail previously.[57−63] On the basis of previous studies, we estimate the proportion of absorbed F-68 to lipid in liposomes is around 1:17 when 0.2 wt % F-68 and 5 mg mL^{-1} egg PC are used in outer and middle phases, respectively (Supplementary Experimental Details 6). Fortunately, the Pluronic F-68 is a nonionic, biocompatible surfactant often used in cell cultures to reduce cell attachment and in drug delivery system. It has been reported that the use of F-68 in liposomes can greatly improve the stability of liposomes for up to 3 months.[64] In our experiments, more than 80% percent of liposome are present after storage for 2 days. The burst liposomes formed small pieces of fragments and aggregates of lipids. Consequently, we believe that the presence of F-68 outside the liposomes does not hinder future applications, but provides certain advantages, such as easier fabrication and better stability.

In Vitro Transcription and Translation in Liposomes. The surfactant-controlled strategy to form a large number of the oil-free monodisperse liposomes with high encapsulation efficiency provides an excellent platform to improve liposome-related research. To demonstrate the potential and to prove their compatibility with biomolecules, we employed the liposomes as cell-like bioreactors to perform in vitro tran-

DOI: 10.1021/jacs.6b02107
J. Am. Chem. Soc. 2016, 138, 7584−7591

scription and translation (IVTT).[6,15,16] Liposomes filled with cell-free gene expression solutions were successfully created using mixtures of *E. coli* extracts, feeding buffer, plasmids coding for enhanced green fluorescent protein (eGFP), and T7 promoters, as inner water phase. As Figure 3a–c show, the

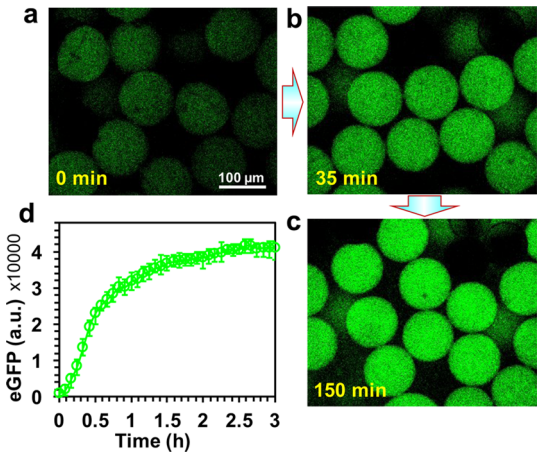

Figure 3. IVTT of eGFP in liposomes. (a–c) Sequence images show expression of eGFP inside the liposomes and (d) the corresponding expression kinetics (average of 30 liposomes).

fluorescence intensity of eGFP in liposomes notably increases from 0 to 35 min and to 150 min. In the first hour, the fluorescence signal increases linearly and then reaches a plateau after 3 h expression probably due to the reaction mixture running out of nutrients. Moreover, the fluorescence intensity increase is similar for all liposomes at the same incubation time. Although residual solvent levels in liposomes are very low and do not prevent the IVTT reaction, one could be concerned about the potentially negative impact of chloroform and hexane on gene expression. Therefore, we performed IVTT of eGFP in a plate reader by adding 4 vol % mixtures of chloroform and hexane (36:64, v/v) in the gene expression solution. We do observe a roughly 25% drop in protein yields, indicating that even at these high concentrations of organic solvents, gene expression is still feasible (Figure S10). Furthermore, during liposome preparation, the oil drops separate from liposomes spontaneously within several minutes and can be removed by exploiting density difference (Figure S3), which minimizes the impact of solvents (Figure S9).

Insertion of Nanopores into Liposomes. The transmembrane transport of molecules and unilamellarity of liposomes are essential in a myriad of fields including artificial cells and membrane protein science. Therefore, to demonstrate that the membranes of the liposomes formed in our methods are bilayers and to show the feasibility of engineering the properties of such membranes, we performed protein pore-mediated transport of molecules across liposome boundaries by using two different membrane proteins, melittin and alpha-hemolysin (αHL). Melittin self-assembles into bilayers to form a pore of 1–3 nm or 3.5–4.5 nm in diameter depending on the number of assembly subunits;[65−67] while αHL only forms nanopore (1.4 nm in diameter) in unilamellar (i.e., single bilayer) membranes.[68] We first prepared liposomes loaded with melittin monomers (2 μM) and calcein fluorescent molecules (10 μM), and observed the fluorescence intensity in liposomes over time. The melittin-induced transport is shown in Figure 4b. Once nanopores were formed, the dye in the liposomes

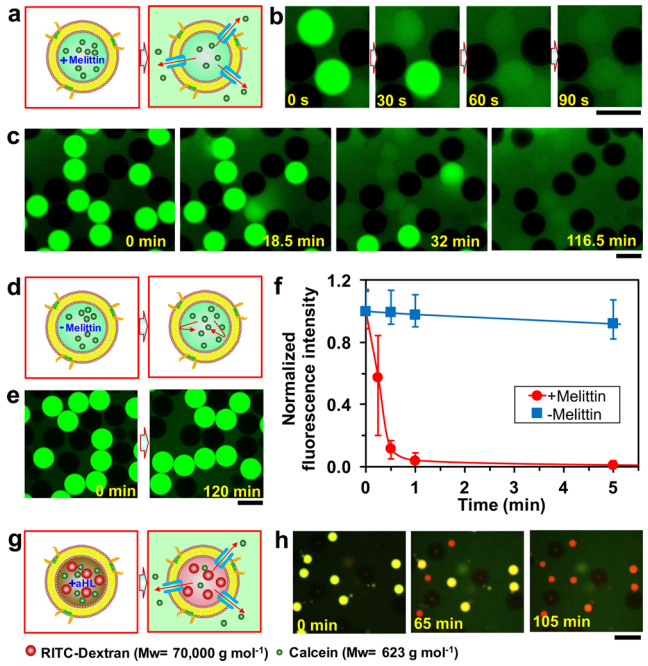

Figure 4. Insertion of melittin and αHL into liposome bilayers. (a) Schematic diagram and (b,c) confocal image series show melittin pore-mediated transport of fluorescent molecules. (d,e) Control experiment: no melittin was added in the liposomes. (f) Kinetics of time-dependent release of calcein fluorescence. In each case, 10 liposomes were measured. (g) Schematic diagram and (h) confocal image series show αHL pore-mediated, selective transport of fluorescent molecules. Small molecule calcein can cross the nanopores, while RITC-Dextran remains in liposomes. All scale bars are 100 μm.

rapidly (<1 min) diffused into the external solution. We note that the releases of molecules from liposomes is not synchronous, which may be a result of the fact the pores do not all form at the same time,[69,70] (Figures 4c and S11). In contrast, in the absence of membrane proteins, liposomes only exhibit slight decay in fluorescence due to photobleaching when observed at the same condition (Figures 4d-f). To further confirm the lamellarity of the liposomes, size exclusion control was performed by insertion of αHL into the membranes (Figures 4g and S12). We encapsulated rhodamine B isothiocyanate-dextran (RITC-Dextran, average M_W = 70 000 g mol^{-1}), calcein (M_W = 623 g mol^{-1}) and αHL in liposomes to observe the selective dye diffusion, because nanopores created by αHL only allow small molecules (less than 2000 g mol^{-1}) to transfer.[6,68] Consequently, these experiments not only demonstrate the membrane unilamellarity of our liposomes, but also show the feasibility of combining diverse nanopores in liposomal systems.

Assembly of Multicompartment Liposomes. The next paragraph we will show how the surfactant-assisted microfluidic method can be easily scaled to fabricate monodisperse liposomes with multicompartments in large quantities. Such liposomes have been formed recently by using a gravity-mediated phase-transfer method.[71] However, poor control over fluid in this manual method leads to liposomes with large sizes, polydisperse structures, low yields and an irreproducible process. Precise manipulation of fluids in microfluidics makes it possible to engineer uniform and small-sized multicompartment liposomes in a well-controlled way. Here we employ the interior water drops of double emulsions as building blocks to

DOI: 10.1021/jacs.6b02107
J. Am. Chem. Soc. 2016, 138, 7584–7591

construct the desired multicompartment liposomes (Figure 5a). To prepare the multicore templates, we used a two-stage device

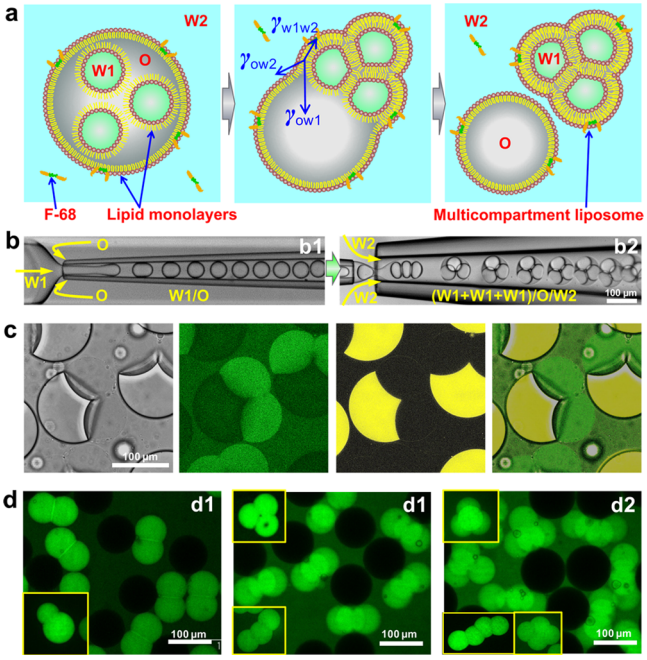

Figure 5. Liposomes with identical multicompartments. (a) Schematic cartoon of surfactant-assisted assembly of multicompartment liposome. (b) Snapshots of fabrication of double emulsions with three interior drops. (c) Confocal images of formation of dual-compartmental liposomes dewetted from dual-core double emulsions; inset in c2 is a liposome with two different sized compartments. (d) Resultant liposomes with three (d1) and four (d2) compartments; insets in d1 and d2 show diverse configurations of liposomes.

to prepare the W1/O droplets at a first stage and sequentially encapsulated them in a second step to form double emulsions with controlled number of inner drops (Figures 5b, S13 and Movie S4). After generation, the lipid-stabilized interior droplets adhere to one another forming bilayers, and then the whole assembly escapes from the oil shell with the assist of F-68 (Figures 5a,c and S14), resulting in multicompartment liposomes (Figure 5d). This process is similar to the dewetting formation of multicompartment polymersomes.[51] By controlling flow rates, double emulsions containing two, three, four and even more than 30 inner drops were created as templates to assemble liposomes with controlled numbers of compartments, and to an extent, a controlled geometry (Figures 5d, S15 and S16). For example, liposomes with three compartments commonly display two configurations, i.e., triangular and linear configurations. To the best of our knowledge, this is the first work that shows controllable preparation of multicompartment liposomes in microfluidics.

Controllable complex multiple emulsions fabricated in microfluidics offer perfect templates to assemble monodisperse structured liposomes with distinct internal compartments.[72] To prove this concept, we upgraded the microfluidic device with two independent droplet generators at the first stage as shown in Figures 6a and S17. The two droplet streams, of which one contains Alexa Fluor 488 dye (W1) and the other contains Alexa Fluor 647 dye (W1′), were paired in a larger microcapillary (Movie S5) and encapsulated into a larger droplet at the second stage to form double emulsions

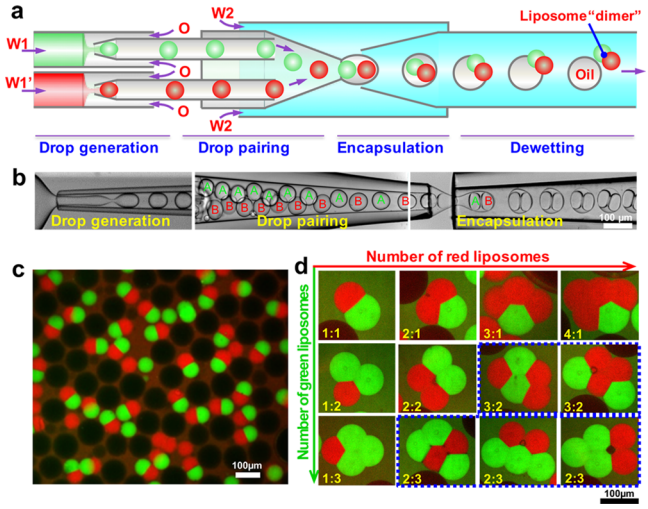

Figure 6. Liposomes with distinct multicompartments. (a,b) Schematic and snapshots of fabrication of double emulsions with two distinct drops. (c) Confocal images of monodisperse liposomes with two different compartments. (d) As-prepared liposomes with controlled structures and various configurations. Scale bars are 100 μm.

containing different droplets (Figures 6b, S17 and Movie S6). This device configuration yielded monodisperse liposomes with two different compartments (liposome "dimers") (Figure 6c). By simply varying relative flow rates, liposomes with a controllable number and type of inner compartments can be formed. The images of liposomes in Figure 6d demonstrates the level of control achieved. For instance, when the green compartment is one, the red compartment can be tuned from one to four or even more. In addition, the yields of the multicompartment structures are also as high as 62% in dual-compartment liposomes (Figure S18). Although the dewetting process is well-controlled and stable, some of the sample were lost because dewetting already started in flowing microchannels which leads to the instability of bilayers. Low flow rates and expanded collection channels would help to increase the yields if required.

Remarkably, when the number of compartments is more than three, the liposomes will exhibit various configurations like liposome "isomers" (framed images in Figure 6d). For example, liposomes containing 1:2 compartments show 3 possible "isomers" (Figure 7a), while liposomes containing 2:2 compartments have as diverse as 11 possible "isomers" (see Figure S19 for several examples). To show the ratio of liposome "iosmers", 220 liposomes containing one red compartment and two green compartments were collected and analyzed. The number distribution of the liposome "trimers" is illustrated in Figure 7a. The number of type B is about twice of that of type C, which agrees well with their formation probabilities.

Hereinabove we have demonstrated the membranes of single liposomes are bilayers. Here we confirm the internal membranes between compartments are also bilayers by insertion of αHL. This is a key step of the multicompartmental structures to successful application in mimicking cell−cell communications and performing coupled multistep micro-reactions. As Figure 7b shows, we loaded a small fluorescent molecule calcein in one compartment, and αHL and a big fluorescent molecule Rhodamine B isothiocyanate−dextran

DOI: 10.1021/jacs.6b02107
J. Am. Chem. Soc. 2016, 138, 7584−7591

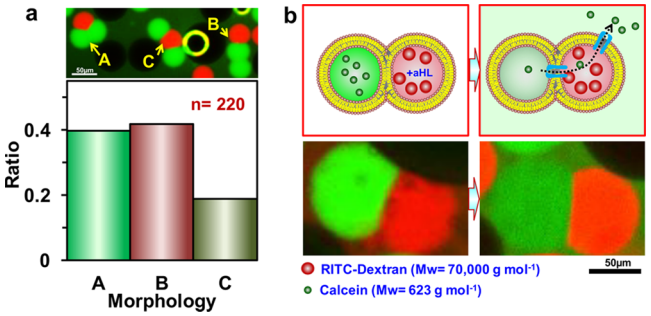

Figure 7. (a) Confocal image of the liposomes with one red compartment and two green compartments showing three different configurations and their ratios counted from 220 liposomes. (b) Schematics and confocal images of insertion of αHL into the intramulticompartment liposome bilayers to selectively release fluorescent molecules.

(RTIC-Dextran) in the other compartment. When the nanopores were created in intramulticompartment liposome membrane and external membrane of RTIC-Dextran dyed liposome, calcein diffused out from the path created by nanopores (Figure 7b), meaning that the membrane between the two compartments is a bilayer as well, which is also supported by the homogeneity of internal and external membranes of the liposomes (Figure S20).

CONCLUSIONS

In conclusion, we have shown a new concept to form monodisperse, complex liposomal structures in microfluidics by using surfactants to control the interfacial energies of W/O/W emulsion drops to induce spontaneous and complete dewetting. By using different surfactant concentrations, we were able to tune the dewetting time from less than 1 min to about 3 h. By using diverse emulsion templates, the dimensions and the number of compartments in the resultant liposomes were all controlled. Finally, we demonstrated that the dewetting approach is compatible with cell-free gene expression and that protein nanopores can be introduced in the unilamellar vesicles. We believe that these liposome networks could have potential as new designs for synergistic delivery systems, synthetic cells for mimicking cell−cell communications, or as coupled multistep microreactors.

EXPERIMENTAL SECTION

Materials. To prepare monodisperse W/O/W double emulsions, an aqueous solution with 8 wt % polyethylene glycol (PEG, M_W = 6000 g mol^{-1}, VWR) and 2 wt % poly(vinyl alcohol) (PVA, M_W = 13 000−23 000 g mol^{-1}, 87−88% hydrolyzed, Sigma-Aldrich), a mixture of chloroform and hexane (30:70, 36:64, 40:60 or 50:50, v/v) containing 1−5 mg mL^{-1} L-α-phosphatidylcholine (egg PC, Avanti Polar Lipids) as well as 10 wt % PVA with 0.1−5.0 wt % Pluronic F-68 (ThermoFisher Scientific) were respectively utilized as inner water phase (W1), middle oil phase (O) and outer water phase (W2). To show the flexibility of this method, other lipids, such as 1,2-dioleoyl-*sn*-glycero-3-phosphocholine (DOPC), 1,2-dimyristoyl-*sn*-glycero-3-phosphocholine (DMPC), 1,2-diphytanoyl-*sn*-glycero-3-phosphocholine (DPhPC) and *E. coli* lipids (all from Avanti Polar Lipids), were tested in our experiments as well. To visualize as-formed liposomes, water-soluble dyes including methylene blue (Sigma-Aldrich), fluorescein isothiocyanate-dextran (FITC-Dextran, M_W = 40 000 g mol^{-1}, Sigma-Aldrich), Alexa Fluor 488 (A488, Invitrogen) and Alexa Fluor 647 (A647) were added in the inner phase and labeled lipids 1,2-dimyristoyl-*sn*-glycero-3-phosphoethanolamine-*N*-(lissamine rhodamine B sulfonyl) (ammonium salt) (Rh-PE) were used in middle phase to show the membrane. To demonstrate the function of F-68 in dewetting process, 10 wt % PVA was used as outer phase to prepare double emulsions without F-68.

Microfluidics. The microfluidic devices are based on coaxial assemblies of round and square glass capillaries on glass slides reported by Weitz group.[73] In brief, two cylindrical capillaries of outer diameter 960 μm, inner diameter 400 μm were precisely tapered to achieve orifice sizes of about 20−50 and 60−100 μm in diameter by using a capillary puller (PN-31, Narishige) and a microforge (MF-830, Narishige). The microcapillary with smaller tip modified by trimethylsilyl chloride (Sigma-Aldrich) into hydrophobic was used for flowing inner phase, while the capillary with larger diameter was treated by 2-[methoxy(polyethyleneoxy)propyl] trimethoxysilane (Gelest, Inc.) to render its surface hydrophilic, and used as the collection tube. Both of two cylindrical capillaries were inserted into a square capillary of inner diameter 1.00 mm from its two opposite ends. The gaps between the square capillary and round capillary are used as two channels for flowing middle and outer phase as shown in Figure 1b. Lastly, dispensing needles used as inlets of fluids were connected at the junctions between capillaries or their ends by using a transparent 5 min Epoxy (Devcon).

To prepare double emulsions with multicores, the devices are scalable to two-stages; i.e., a flow-focusing drop generator is designed at the first stage. In short, a cylindrical microcapillary of outer diameter 170 μm was engineered into approximately 30 μm at one end that was inserted into a square microcapillary of inner diameter 200 μm to form a drop generator. The collection tube in first stage, that is, the other unprocessed end of the round microcapillary was inserted into the inlet of cylindrical microcapillary (inner diameter 400 μm) at the second stage, which is fabricated as described hereinabove. To prepare double emulsions with two distinct interior drops, devices with two flow-focusing drop generators at the first stage were designed and fabricated similarly.

To generate the double emulsions, all fluids were pumped into the capillary microfluidic devices by using syringe pumps (PHD 2000 series, Harvard Apparatus) at desired flow rates. Typical flow rates of the inner, middle and outer phases are 500, 500, and 2000−5000 μL h^{-1}, respectively. The formation process of emulsion drops were monitored by using an inverted optical microscope (IX71, Olympus) equipped with a high-speed camera (Miroex4, Phantom, Vision Research). The freshly prepared emulsions were collected in a semienclosed silicone isolation chamber (diameter 9 mm, height 0.12 mm, SecureSeal) covered with a glass coverslide for further characterization. The dewetting process and resultant labeled liposomes were observed by an optical microscope (IX81, Olympus) and a confocal laser scanning microscope (CLSM) (SP8x, Leica).

Removal of Residual Oil Droplets. To remove the residual oil droplets in as-formed liposome samples, we exploit their density differences (Figure S3). Briefly, the freshly prepared mixtures of liposomes (density 1.017 g mL^{-1}) and residual oil droplets (density of 30:70 chloroform and hexane, less than 0.905 g mL^{-1}) were collected in a container (for example, a vial) that contains an isotonic solution (as inside of liposome) whose density is between those of liposome and oil droplet, such as sucrose or salt solution. For demonstration, we injected the mixtures into 100 mM sucrose solution (density, 1.010 g mL^{-1}). As expected, oil droplets floated into the top of sucrose solution, while liposomes settled down at the bottom of the vial. Lastly, the floating oil droplets can be easily removed by pipetting or evaporating, resulting in pure liposome samples in vial (Figure S3).

IVTT in Liposomes. The transcription-translation reaction mixtures mainly consisted of one-third *Escherichia coli* cell lysate (100 μL) and two-thirds feeding buffer (200 μL), which were prepared and stored according to recent publication of our group.[74] Before preparing liposomes, T7 RNA polymerases (63 U) and plasmids coding for enhanced green fluorescent protein (eGFP) (3 nM) were supplemented to the mixture in a cold room, then the final mixture was used as inner phase to fabricate loaded liposomes. The collected liposomes were incubated at room temperature (about 22 °C) and monitored for 4 h by an inverted microscope (IX81, Olympus) equipped with a sensitive EMCCD camera (iXon3; Andor). The

DOI: 10.1021/jacs.6b02107
J. Am. Chem. Soc. 2016, 138, 7584−7591

detection interval was 5 min and the laser exposure time was 500 ms. Images showing fluorescence intensity of eGFP inside the liposomes were analyzed by a free software ImageJ.

Membrane Protein Insertion Assay. To incorporate the membrane protein into the liposomes, melittin (2 μM) or αHL (10 μg mL^{-1}) together with calcein (10 μM, pH 7.35, M_W = 623 g mol^{-1}) or Rhodamine B isothiocyanate−dextran (10 μM, RTIC-Dextran, M_W = 70 000 g mol^{-1}) were loaded in the inner phase to prepare liposomes. Commercial lyophilized powder of melittin or α-HL (Sigma-Aldrich) was first solubilized in milli-Q water, and then added into W1 phase to desired concentrations. As-formed liposomes were collected in a semienclosed silicone isolation chamber, and then recorded automatically by an inverted microscope (IX81, Olympus) equipped with a sensitive EMCCD camera (iXon3; Andor) illuminating from a mercury lamp. The interval time of detection was 0.5 min and the mercury lamp exposure time was 250 ms. Images were processed and analyzed by ImageJ.

Measurement of Interfacial Energies. In W1/O/W2 emulsion system, the interfacial tensions between O−W1 phases and that between O−W2 phases (immiscible phases) were measured by a drop shape analysis system (FTA 1000, First Ten Angstroms) using pendant drop method at room temperature. Since there is no direct method to measure the interfacial tension of bilayer membrane between two water phases, here we performed an adhesion experiment of two lipid-stabilized water drops to calculate the interfacial tension according to force balance (see Supporting Information). Briefly, W1/O drops and W2/O drops were simultaneously generated in two single-staged capillary microfluidic devices, respectively. The two kinds of piled drops were collected in a same container to make them contact sufficiently. Then their configurations were recorded by an optical microscope (BX 71, Olympus) for further calculation.

■ ASSOCIATED CONTENT

Supporting Information

The Supporting Information is available free of charge on the ACS Publications website at DOI: 10.1021/jacs.6b02107.

Supplementary experimental details show the measurement and analysis of interfacial energies as well as characterization of resultant liposomes; supplementary figures and movies show fabrication of diverse emulsion templates and liposomes as well as membrane protein-mediated transport of fluorescence molecules. (PDF)

Movie S1. (AVI)

Movie S2. (AVI)

Movie S3. (AVI)

Movie S4. (AVI)

Movie S5. (AVI)

Movie S6. (AVI)

■ AUTHOR INFORMATION

Corresponding Author

*w.huck@science.ru.nl

Notes

The authors declare no competing financial interest.

■ ACKNOWLEDGMENTS

This work was supported by the European Research Council (ERC, advanced grant 246812 Intercom, to W.T.S.H.), The Netherlands Organization for Scientific Research (NWO, VICI grant 700.10.44, to W.T.S.H.), the Ministry of Education, Culture and Science (Gravity programme, 024.001.035), and a Marie Skłodowska-Curie Actions Individual Fellowships (EC, H2020-MSCA-IF grant 659907, to N.-N.D.).

■ REFERENCES

(1) Torchilin, V. P. *Nat. Rev. Drug Discovery* **2005**, *4*, 145−160.

(2) Pattni, B. S.; Chupin, V. V.; Torchilin, V. P. *Chem. Rev.* **2015**, *115*, 10938−10966.

(3) Zimmerberg, J.; Kozlov, M. M. *Nat. Rev. Mol. Cell Biol.* **2006**, *7*, 9−19.

(4) Bangham, A. D.; Hill, M. W.; Miller, N. G. A. In *Methods in Membrane Biology*; Korn, E. D., Ed.; Springer US: Boston, MA, 1974; Vol. *1*, pp 1−68.

(5) Früh, V.; Ijzerman, A. P.; Siegal, G. *Chem. Rev.* **2011**, *111*, 640−656.

(6) Noireaux, V.; Libchaber, A. *Proc. Natl. Acad. Sci. U. S. A.* **2004**, *101*, 17669−17674.

(7) Mansy, S. S.; Schrum, J. P.; Krishnamurthy, M.; Tobe, S.; Treco, D. A.; Szostak, J. W. *Nature* **2008**, *454*, 122−125.

(8) Bolinger, P.-Y.; Stamou, D.; Vogel, H. *J. Am. Chem. Soc.* **2004**, *126*, 8594−8595.

(9) Bally, M.; Bailey, K.; Sugihara, K.; Grieshaber, D.; Vörös, J.; Städler, B. *Small* **2010**, *6*, 2481−2497.

(10) Zhou, J.; Wang, Q.-x.; Zhang, C.-y. *J. Am. Chem. Soc.* **2013**, *135*, 2056−2059.

(11) Adamala, K.; Szostak, J. W. *Science* **2013**, *342*, 1098−1100.

(12) Chen, I. A.; Salehi-Ashtiani, K.; Szostak, J. W. *J. Am. Chem. Soc.* **2005**, *127*, 13213−13219.

(13) Oberholzer, T.; Wick, R.; Luisi, P. L.; Biebricher, C. K. *Biochem. Biophys. Res. Commun.* **1995**, *207*, 250−257.

(14) Oberholzer, T.; Albrizio, M.; Luisi, P. L. *Chem. Biol.* **1995**, *2*, 677−682.

(15) Saito, H.; Kato, Y.; Le Berre, M.; Yamada, A.; Inoue, T.; Yosikawa, K.; Baigl, D. *ChemBioChem* **2009**, *10*, 1640−1643.

(16) Nishimura, K.; Matsuura, T.; Nishimura, K.; Sunami, T.; Suzuki, H.; Yomo, T. *Langmuir* **2012**, *28*, 8426−8432.

(17) Szostak, J. W.; Bartel, D. P.; Luisi, P. L. *Nature* **2001**, *409*, 387−390.

(18) Noireaux, V.; Maeda, Y. T.; Libchaber, A. *Proc. Natl. Acad. Sci. U. S. A.* **2011**, *108*, 3473−3480.

(19) Osawa, M.; Anderson, D. E.; Erickson, H. P. *Science* **2008**, *320*, 792−794.

(20) Osawa, M.; Erickson, H. P. *Proc. Natl. Acad. Sci. U. S. A.* **2013**, *110*, 11000−11004.

(21) Terasawa, H.; Nishimura, K.; Suzuki, H.; Matsuura, T.; Yomo, T. *Proc. Natl. Acad. Sci. U. S. A.* **2012**, *109*, 5942−5947.

(22) Deshpande, S.; Caspi, Y.; Meijering, A. E. C.; Dekker, C. *Nat. Commun.* **2016**, *7*, 10447.

(23) Kurihara, K.; Okura, Y.; Matsuo, M.; Toyota, T.; Suzuki, K.; Sugawara, T. *Nat. Commun.* **2015**, *6*, 8352.

(24) Kurihara, K.; Tamura, M.; Shohda, K.-i.; Toyota, T.; Suzuki, K.; Sugawara, T. *Nat. Chem.* **2011**, *3*, 775−781.

(25) Rossier, O.; Cuvelier, D.; Borghi, N.; Puech, P. H.; Derényi, I.; Buguin, A.; Nassoy, P.; Brochard-Wyart, F. *Langmuir* **2003**, *19*, 575−584.

(26) Montes, L. R.; Alonso, A.; Goñi, F. M.; Bagatolli, L. A. *Biophys. J.* **2007**, *93*, 3548−3554.

(27) Szoka, F.; Papahadjopoulos, D. *Proc. Natl. Acad. Sci. U. S. A.* **1978**, *75*, 4194−4198.

(28) Pautot, S.; Frisken, B. J.; Weitz, D. A. *Proc. Natl. Acad. Sci. U. S. A.* **2003**, *100*, 10718−10721.

(29) Li, S.; Palmer, A. F. *Langmuir* **2004**, *20*, 7917−7925.

(30) Hishida, M.; Seto, H.; Yamada, N. L.; Yoshikawa, K. *Chem. Phys. Lett.* **2008**, *455*, 297−302.

(31) Rodriguez, N.; Pincet, F.; Cribier, S. *Colloids Surf., B* **2005**, *42*, 125−130.

(32) Walde, P.; Cosentino, K.; Engel, H.; Stano, P. *ChemBioChem* **2010**, *11*, 848−865.

(33) van Swaay, D.; deMello, A. *Lab Chip* **2013**, *13*, 752−767.

(34) Hu, P. C.; Li, S.; Malmstadt, N. *ACS Appl. Mater. Interfaces* **2011**, *3*, 1434−1440.

(35) Matosevic, S.; Paegel, B. M. *J. Am. Chem. Soc.* **2011**, *133*, 2798−2800.

DOI: 10.1021/jacs.6b02107
J. Am. Chem. Soc. 2016, 138, 7584−7591

(36) Tan, Y.-C.; Hettiarachchi, K.; Siu, M.; Pan, Y.-R.; Lee, A. P. *J. Am. Chem. Soc.* **2006**, *128*, 5656−5658.
(37) Abkarian, M.; Loiseau, E.; Massiera, G. *Soft Matter* **2011**, *7*, 4610−4614.
(38) Shum, H. C.; Lee, D.; Yoon, I.; Kodger, T.; Weitz, D. A. *Langmuir* **2008**, *24*, 7651−7653.
(39) Arriaga, L. R.; Datta, S. S.; Kim, S.-H.; Amstad, E.; Kodger, T. E.; Monroy, F.; Weitz, D. A. *Small* **2014**, *10*, 950−956.
(40) Funakoshi, K.; Suzuki, H.; Takeuchi, S. *J. Am. Chem. Soc.* **2007**, *129*, 12608−12609.
(41) Stachowiak, J. C.; Richmond, D. L.; Li, T. H.; Liu, A. P.; Parekh, S. H.; Fletcher, D. A. *Proc. Natl. Acad. Sci. U. S. A.* **2008**, *105*, 4697−4702.
(42) Ota, S.; Yoshizawa, S.; Takeuchi, S. *Angew. Chem., Int. Ed.* **2009**, *48*, 6533−6537.
(43) Lee, S. S.; Abbaspourrad, A.; Kim, S.-H. *ACS Appl. Mater. Interfaces* **2014**, *6*, 1294−1300.
(44) Deng, N.-N.; Sun, J.; Wang, W.; Ju, X.-J.; Xie, R.; Chu, L.-Y. *ACS Appl. Mater. Interfaces* **2014**, *6*, 3817−3821.
(45) Beales, P. A.; Vanderlick, T. K. *Adv. Colloid Interface Sci.* **2014**, *207*, 290−305.
(46) Elani, Y.; Law, R. V.; Ces, O. *Nat. Commun.* **2014**, *5*, 5305.
(47) Karlsson, A.; Karlsson, R.; Karlsson, M.; Cans, A.-S.; Stromberg, A.; Ryttsen, F.; Orwar, O. *Nature* **2001**, *409*, 150−152.
(48) Karlsson, M.; Sott, K.; Davidson, M.; Cans, A.-S.; Linderholm, P.; Chiu, D.; Orwar, O. *Proc. Natl. Acad. Sci. U. S. A.* **2002**, *99*, 11573−11578.
(49) Villar, G.; Graham, A. D.; Bayley, H. *Science* **2013**, *340*, 48−52.
(50) Villar, G.; Heron, A. J.; Bayley, H. *Nat. Nanotechnol.* **2011**, *6*, 803−808.
(51) Shum, H. C.; Zhao, Y.-j.; Kim, S.-H.; Weitz, D. A. *Angew. Chem., Int. Ed.* **2011**, *50*, 1648−1651.
(52) Shum, H. C.; Kim, J.-W.; Weitz, D. A. *J. Am. Chem. Soc.* **2008**, *130*, 9543−9549.
(53) Shum, H. C.; Santanach-Carreras, E.; Kim, J.-W.; Ehrlicher, A.; Bibette, J.; Weitz, D. A. *J. Am. Chem. Soc.* **2011**, *133*, 4420−4426.
(54) Torza, S.; Mason, S. G. *Science* **1969**, *163*, 813−814.
(55) Deng, N.-N.; Wang, W.; Ju, X.-J.; Xie, R.; Weitz, D. A.; Chu, L.-Y. *Lab Chip* **2013**, *13*, 4047−4052.
(56) Thiam, A. R.; Bremond, N.; Bibette, J. *Phys. Rev. Lett.* **2011**, *107*, 068301.
(57) McIntosh, T. J.; Magid, A. D.; Simon, S. A. *Biochemistry* **1989**, *28*, 7904−7912.
(58) Firestone, M. A.; Wolf, A. C.; Seifert, S. *Biomacromolecules* **2003**, *4*, 1539−1549.
(59) Heerklotz, H. H.; Binder, H.; Epand, R. M. *Biophys. J.* **1999**, *76*, 2606−2613.
(60) Johnsson, M.; Silvander, M.; Karlsson, G.; Edwards, K. *Langmuir* **1999**, *15*, 6314−6325.
(61) Kostarelos, K.; Tadros, T. F.; Luckham, P. F. *Langmuir* **1999**, *15*, 369−376.
(62) Wu, G.; Khant, H. A.; Chiu, W.; Lee, K. Y. C. *Soft Matter* **2009**, *5*, 1496−1503.
(63) Wu, G.; Majewski, J.; Ege, C.; Kjaer, K.; Weygand, M. J.; Lee, K. Y. *Biophys. J.* **2005**, *89*, 3159−3173.
(64) Teh, S.-Y.; Khnouf, R.; Fan, H.; Lee, A. P. *Biomicrofluidics* **2011**, *5*, 044113.
(65) Andreeva-Kovalevskaya, Z. I.; Solonin, A. S.; Sineva, E. V.; Ternovsky, V. I. *Biochemistry (Moscow)* **2008**, *73*, 1473−1492.
(66) Matsuzaki, K.; Yoneyama, S.; Miyajima, K. *Biophys. J.* **1997**, *73*, 831−838.
(67) Ladokhin, A. S.; Selsted, M. E.; White, S. H. *Biophys. J.* **1997**, *72*, 1762−1766.
(68) Song, L.; Hobaugh, M. R.; Shustak, C.; Cheley, S.; Bayley, H.; Gouaux, J. E. *Science* **1996**, *274*, 1859−1865.
(69) Leptihn, S.; Castell, O. K.; Cronin, B.; Lee, E.-H.; Gross, L. C. M.; Marshall, D. P.; Thompson, J. R.; Holden, M.; Wallace, M. I. *Nat. Protoc.* **2013**, *8*, 1048−1057.
(70) Holden, M. A.; Needham, D.; Bayley, H. *J. Am. Chem. Soc.* **2007**, *129*, 8650−8655.
(71) Elani, Y.; Gee, A.; Law, R. V.; Ces, O. *Chem. Sci.* **2013**, *4*, 3332−3338.
(72) Wang, W.; Xie, R.; Ju, X.-J.; Luo, T.; Liu, L.; Weitz, D. A.; Chu, L.-Y. *Lab Chip* **2011**, *11*, 1587−1592.
(73) Utada, A. S.; Lorenceau, E.; Link, D. R.; Kaplan, P. D.; Stone, H. A.; Weitz, D. A. *Science* **2005**, *308*, 537−541.
(74) Sokolova, E.; Spruijt, E.; Hansen, M. M. K.; Dubuc, E.; Groen, J.; Chokkalingam, V.; Piruska, A.; Heus, H. A.; Huck, W. T. S. *Proc. Natl. Acad. Sci. U. S. A.* **2013**, *110*, 11692−11697.

DOI: 10.1021/jacs.6b02107
J. Am. Chem. Soc. 2016, 138, 7584−7591